Contributions of intrinsic and synaptic activities to the generation of neuronal discharges in *in vitro* hippocampus

Ivan Cohen and Richard Miles

Laboratoire de Neurobiologie Cellulaire, INSERM U261, Institut Pasteur, 25 rue de Dr Roux, 75724 Paris cedex 15, France

(Received 9 September 1999; accepted after revision 17 January 2000)

1. Extracellular and intracellular records were made from guinea-pig hippocampal slices to examine the contributions of intrinsic cellular properties and synaptic events to the generation of neuronal activity. Extracellular signals were filtered to pass action potentials, which could be detected within a distance of about 80 μm from a discharging cell.

2. Spontaneous action potentials were invariably detected in records from the stratum pyramidale of CA3 region. Blocking excitatory synaptic transmission with NBQX and APV reduced their frequency by $23 \pm 35\,\%$. Suppressing synaptic inhibition, while excitation was already blocked, increased the rate of spike discharge to $177 \pm 71\,\%$ of its control value.

3. Most action potentials recorded intracellularly from CA3 pyramidal cells were initiated in the absence of a detectable synaptic event. In contrast, most action potentials generated by inhibitory cells located close to stratum pyramidale were preceded by an EPSP.

4. In 31 simultaneous recordings, intracellular pyramidal cell action potentials appeared consistently to initiate extracellular spikes with a mean latency of $2{\cdot}2 \pm 1{\cdot}0$ ms. Single inhibitory cell action potentials could initiate a reduction in the frequency of extracellular spikes of duration 10–30 ms.

5. Some identified extracellular spikes ($n = 9$) consistently preceded intracellularly recorded IPSPs. IPSPs were initiated monosynaptically with latencies of 0·9–1·5 ms. In reciprocal interactions, single pyramidal cell action potentials could trigger the discharge of an identified unit that in turn appeared to initiate an IPSP in the same pyramidal cell.

6. These data suggest that intrinsic cellular mechanisms underly much of the spontaneous activity of pyramidal cells of the CA3 region of the hippocampus *in vitro*. Both synaptic inhibition and a strong excitation of inhibitory cells by pyramidal cells act to reduce population activity.

Activity in a neuronal network may depend on afferent signalling or result from processes intrinsic to the network. *In vitro* studies suggest that some brain areas may generate discharges in the absence of external inputs. Both intrinsic cellular properties and synaptic connections within the network could contribute to this activity. However, the relative contributions of autonomous neuronal firing and of inhibitory and excitatory synaptic circuits are not clear. Records from pairs of connected cells have increased our understanding on inhibitory and excitatory synaptic interactions within cortical networks (Gulyás *et al.* 1993; Buhl *et al.* 1994; Miles & Poncer, 1996; Markram *et al.* 1997). But, to examine how synapses between cells embedded in a neuronal network participate in the generation and control of population activity, a sensitive index of activity in neuronal ensembles is needed (Churchland & Sejnowski, 1988).

Most available techniques to measure neuronal population activities either lack spatial or temporal resolution or cannot resolve discharges in a useful number of cells. Ensemble activity has been measured as field potentials (Schwartzkroin & Prince, 1978) which reflect both synchronous synaptic events and cellular discharges. However, the technique is rather insensitive since field potentials emerge only when a large fraction of a neuronal population discharges simultaneously (Miles & Wong, 1987; Prince & Tseng, 1993; Whittington *et al.* 1995). Spontaneous synaptic events – EPSPs or IPSPs – recorded from one or more cells (Miles & Wong, 1987; Mintz & Korn, 1991) provide an index of population activity as they reveal the timing of firing in many presynaptic excitatory or inhibitory cells. However, the location and the number of cells that initiate the synaptic events remain unknown. Finally, optical probes for membrane potential or intracellular calcium have been used to examine neuronal ensemble activity. But these techniques do not yet provide large signals from many separate neurons with the

millisecond time resolution needed to follow spike discharges (Nelson & Katz, 1995).

An older technique is to record extracellular action potentials from a local neuronal population by selectively filtering signals from metal electrodes (Hubel, 1957; Baldwin *et al.* 1965; Buzsáki, 1984; Welsh *et al.* 1995). Extracellular records of action potentials have helped resolve mechanisms of neuronal synchrony in the retina (Meister *et al.* 1991) and thalamus (Kim *et al.* 1995) *in vitro*. However, it is difficult to assign signals to specified cells (McNaughton *et al.* 1983) and to know how many cells may potentially be recorded by a single electrode.

In the present study we used uninsulated electrodes to maximise the number of cells from which an electrode could record. We show that in a hippocampal slice this number is 400–500 pyramidal cells. Using this signal – the action potential activity generated by a local group of neurons – we attempted to dissect contributions of intrinsic and synaptic mechanisms to the generation of hippocampal population activity. Three approaches were used. First, extracellular records demonstrate how firing in a local ensemble of cells changes during pharmacological manipulations of pre- or postsynaptic function at excitatory or inhibitory synapses. Second, we examined with intracellular records how excitatory and inhibitory synaptic events influence pyramidal and inhibitory cell discharges. Finally, intracellular and extracellular records were combined to determine how firing in a single cell influences activity in a larger neuronal ensemble and, reciprocally, the effects of population activity on a single neuron.

METHODS

Hippocampal slices were prepared according to local regulations from guinea-pigs (weight 100–200 g) anaesthetised by intraperitoneal injection of ketamine (200 mg kg^{-1}) and chloral hydrate (800 mg kg^{-1}). Animals were perfused intracardially with a cold (3–5 °C) solution containing 26 mM $NaHCO_3$, 1 mM KCl, 10 mM $MgCl_2$, 1 mM $CaCl_2$, 248 mM sucrose and 10 mM glucose. Animals were killed by decapitation, both hippocampi were dissected free and four to six slices of thickness 450 μm were cut in the same sucrose-containing solution using a vibratome.

The slices were maintained at 34–36 °C in an interface recording chamber. They were perfused with a solution containing 124 mM NaCl, 26 mM $NaHCO_3$, 4 mM KCl, 2 mM $MgCl_2$, 2 mM $CaCl_2$ and 10 mM glucose, equilibrated with 5% CO_2 in 95% O_2. In some experiments the concentration of extracellular K^+ was varied (between 2 and 8 mM). In other experiments drugs affecting receptors at excitatory and inhibitory synapses were added to the perfusing solution. We used 2,3-dioxo-6-nitro-1,2,3,4-tetrahydrobenzo-quinoxaline-7-sulphonamide (3–5 μM, NBQX) and D,L-2-amino-5-phosphonovaleric acid (100 μM, APV) to block fast EPSPs. Picrotoxin (50 μM) or bicuculline (10 μM) were used to block fast $GABA_A$ receptor-mediated IPSPs. In some experiments lower concentrations of bicuculline (0·5–2·5 μM) were used to reduce the efficacy of fast synaptic inhibition. We also examined the effects of the group III metabotropic glutamate receptor agonist L(+)-2-amino-4-phosphonobutyric (L-AP4; 100–150 μM) and of *RS*-α-methyl-4-carboxyphenylglycine (MCPG, 500 μM) and atropine (20 μM), antagonists of metabotropic receptors for glutamate and muscarinic receptors, respectively. NBQX and APV were obtained from Tocris Cookson and other drugs from Sigma.

Glass microelectrodes filled with 2 M potassium acetate and bevelled to final resistances of 40–80 MΩ were used to make intracellular recordings. Membrane potentials were measured using an Axoclamp 2B amplifier. Electrodes for extracellular recording were made from tungsten wire of diameter 50 μm. Their tips were etched to a point of diameter of 2–6 μm under a dissecting microscope, by passing an alternating current (1–5 V for 1–2 min) between the tungsten wire and a carbon electrode immersed in 5 M KNO_2. These electrodes were not insulated and their resistance in physiological solution was 500–1000 kΩ. Up to four electrodes were mounted on holders controlled by separate manipulators. Differences in potential between each tungsten electrode and a reference Ag–AgCl electrode were measured using a 4-channel amplifier (Knight Industrial Technologies, Miami, FL, USA). Signals were amplified 2000 or 5000 times and were filtered (4-pole Bessel with a pass band between 300 and 5000 Hz) so that action potentials were passed. Recording noise with an electrode placed in the perfusing solution was typically 7–15 μV peak-to-peak, while the amplitudes of action potentials recorded from the CA3 stratum pyramidale ranged from this noise level up to about 200 μV.

Signals were stored on a modified videotape recorder (Neurodata, New York, USA). They were digitised at 10–20 kHz, with voltage resolution of 0·6 μV for extracellular signals and 25 μV for intracellular signals, using a 12-bit, 16-channel analog-to-digital converter (Digidata 1200A, Axon Instruments) interfaced to a PC. Signals were visualised on an oscilloscope using the program Axoscope (Axon Instruments).

Action potential frequency and timing, were derived from extracellular signals with software written in the Labview programming language (National Instruments, Austin, TX, USA). Although their shape varied, extracellular spikes always possessed a rapid rising phase. This was used as the basis of our detection algorithm (Fig. 1) which treated extracellular signals to reveal rapidly rising transients with the 'up-only' filter:

$$g(t + \mathrm{d}t) = \begin{cases} g(t) + \mathrm{d}f & [\mathrm{d}f \geqslant 0] \\ 0 & [\mathrm{d}f \leqslant 0] \end{cases}$$

where f is the original signal, g the filtered signal and t is time. This algorithm produced a signal similar to the original during the rising phase of extracellular spikes and close to zero elsewhere. Action potentials were then detected by applying a threshold to the amplitude and slope of the transformed signal. Events were not prolonged by the transform so that detection of nearly coincident spikes was not compromised – near collisions with time differences as short as 2 ms could be resolved. Comparison of the algorithm with visual spike detection suggested that 98–99% of events with amplitudes greater than or equal to 2 times the baseline noise were detected.

In some experiments we examined the influence of firing induced in intracellularly recorded pyramidal or inhibitory cells on summed extracellular unit activity. For this purpose, Parzen estimation (Sanderson & Kobler, 1976; Stricker *et al.* 1994) was used to determine the probability density function of the timing of all detected extracellular spikes with respect to intracellular action potentials. This provided a spike-triggered average of the instantaneous frequency of extracellular activity. Extracellular traces were aligned on intracellular action potentials and unit

discharges were detected and convolved with a Gaussian weighting function. Normalising the sum of all convolved traces provided an averaged instantaneous frequency. The standard deviation of the Gaussian weighting was set at 1–3 ms, depending on the number of traces available to estimate the distribution. Cumulative fluctuations around the baseline frequency were compared before and after the intracellular action potential to determine whether a cell had an effect on population activity. The strength of interactions was quantified as a probability, P, from the integral of the difference between the instantaneous frequency curve and its mean value before the triggering action potential:

$$P = \int_{t_1}^{t_2} (f(t) - f_0) \mathrm{d}t,$$

where $f(t)$ is the instantaneous frequency curve, f_0 the mean background frequency before intracellular firing and t_1 and t_2 the times corresponding to an increase of $f(t)$ by more than 5% above baseline. This gave the probability that a spike occurred in any of the population of extracellularly recorded cells, neglecting collisions. Artefacts corresponding to intracellular action potentials were sometimes evident in extracellular traces. These artefacts were subtracted after determining coupling between channels by applying a best linear estimator over the complete recording. Data are presented as means ± S.D. Significance tests are based on Student's t test. Programming details are available on request from icohen@pasteur.fr.

In one series of experiments we examined how the extracellular action potential signal detected by a tungsten electrode varied with the distance between the electrode and a discharging cell. This was done under visual control (40 × water immersion objective lens, Axioscope IID microscope) by making simultaneously a whole cell recording from a pyramidal cell and an extracellular recording with a tungsten electrode. In these experiments hippocampal slices of thickness 200–250 μm were used. Whole cell recording pipettes had resistances of 3–5 MΩ and contained (mM): 120 potassium gluconate, 10 Hepes, 10 EGTA, 3 $CaCl_2$, 2 $MgCl_2$, 4 $ATP(Na)_2$, 0·4 GTP(Na), 10 KCl (pH adjusted to 7·4 with KOH and osmolarity to 290 mosmol l^{-1}). Depolarising current was injected via an Axoclamp 2B amplifier, operated in current clamp mode, to generate pyramidal cell action potentials, and changes in the corresponding extracellular signal were examined as the separation between the cell and the tip of the extracellular electrode was varied.

RESULTS

Calibration of extracellular recordings

Extracellular signals generated by single neurons were first explored by making simultaneous intra- and extracellular records under visual control. Whole cell records were obtained from single pyramidal cells that were made to discharge single action potentials by current injection. A tungsten electrode placed close to the soma and orthogonal to the major dendritic axis of the recorded pyramidal cell (Fig. 2) detected a signal similar to the second differential with time of the intracellular action potential (Lorente de Nò, 1947; Hubbard *et al.* 1969). Moving the tungsten electrode away from the pyramidal cell soma reduced the amplitude of this signal. Combining results from six dual recordings, we constructed a curve relating the peak-to-peak amplitude of the averaged extracellular signal to the distance between the cell soma and the tungsten electrode (Fig. 2*C*). The extracellular spike amplitude was about 60 μV at a distance of 20 μm and was reduced to about 10 μV at a separation of about 80 μm. Since 10 μV was a typical noise level, a distance of 80 μm can be taken as the spatial limit for reliable signal detection. This permits an estimate for the number of pyramidal cells that an extracellular electrode might record. Using a microscope and a CCD camera calibrated against a micrometre scale, the diameter of CA3 pyramidal cell somata was measured as 18 ± 3 μm ($n = 20$). The mean number of pyramidal somata intersected by a perpendicular line between the borders of the CA3 stratum pyramidale was 3·1 ± 0·8. Thus a tungsten electrode could potentially detect spikes from 400–500 cells in the CA3 stratum pyramidale of a 400 μm thick hippocampal slice.

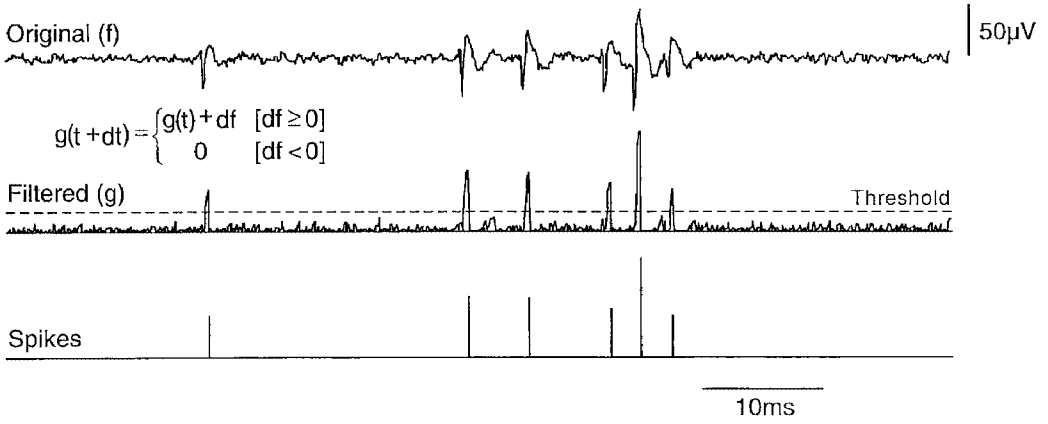

Figure 1. Detection of extracellular spikes

Extracellular signals (top trace) were passed through an 'up-only' digital filter generating a signal (middle trace) that retained the fast spike rising phase. The filter used the formula shown in the inset, with f the original signal, g the processed trace and $\mathrm{d}t$ the time step. For each $\mathrm{d}t$ value, g was increased by $\mathrm{d}f$ when $\mathrm{d}f$ was positive, but was null when $\mathrm{d}f$ was negative. A threshold applied to both the amplitude and rate of rise of the filtered signal permitted measurement of both the timing and the amplitude of detected spikes (bottom trace). Note that three discrete spikes were extracted from the final group of three events.

Extracellular unit activity

Unit activity was always apparent in extracellular records from the stratum pyramidale of the CA3 region (Fig. 3*A*). Spike amplitudes ranged from the noise level up to 50–150 μV, suggesting that electrodes detected discharges from multiple neurons. The frequency of detected spikes, in 20 representative slices, was 40 ± 26 spikes s^{-1}. Usually one or more large amplitude spikes with stereotyped amplitude and form occurred repetitively. These discharges were presumed to be generated by a single neuron and their frequency in the same 20 slices, was $2{\cdot}5 \pm 2{\cdot}6$ spikes s^{-1}.

While most identifiable spikes occurred regularly, two forms of irregular discharge were observed. The first was bursts of three to six spikes, typically with descending amplitude and stereotyped interspike intervals of 5–12 ms. Less frequently, spikes of similar shape and amplitude occurred regularly during periods of several seconds separated by silent periods of similar duration.

In records from the CA1 stratum pyramidale ($n = 8$) and from the dentate gyrus ($n = 6$), there was typically no spontaneous activity, although vertical movement of the recording electrode usually provoked transient firing (Fig. 3*A*). This suggests that dentate granule and CA1 pyramidal cells are less excitable than those in the CA3 region. We compared discharges recorded from the CA1 and CA3 fields ($n = 5$) while extracellular K^+ was changed in the range of 2–8 mM. Firing in the CA3 region persisted as K^+ was lowered to 2 mM and increased in frequency as $K^+$was augmented to 8 mM (Fig. 3*B*). In contrast, extracellular spikes were not apparent in the CA1 stratum pyramidale until $K^+$was increased to 6 mM.

Analysis of spike discharges recorded at different levels of K^+ suggests that increasing K^+ probably recruited previously inactive CA3 neurons to fire as well as increasing the discharge frequency of spontaneously active cells. Figure 3*C* shows amplitude histograms for activity recorded at 2 mM

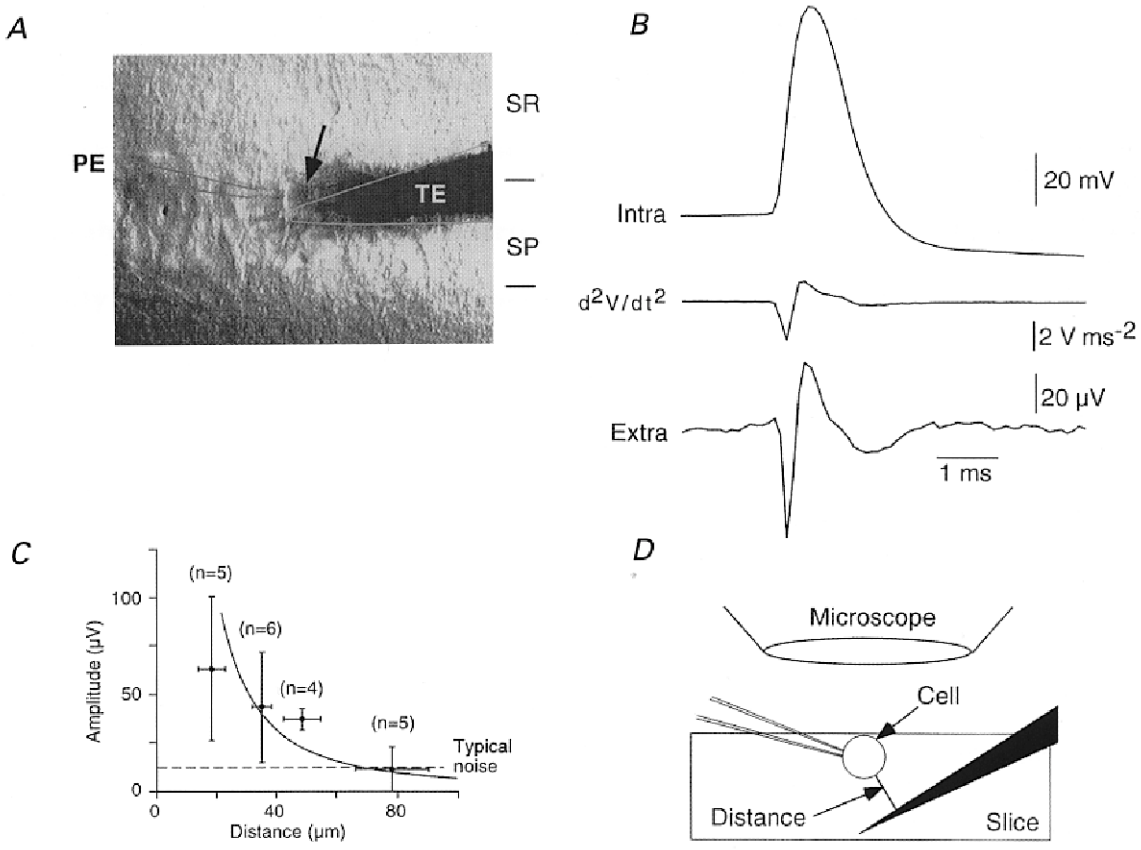

Figure 2. Calibration of extracellular recording electrodes

A, simultaneous whole cell and extracellular records were made under visual control with a patch electrode, PE, and a tungsten extracellular electrode, TE. An arrow shows the recorded cell. SR and SP correspond to s. radiatum and s. pyramidale. *B*, averages ($n = 50$) of intracellular action potentials initiated by current injection into a CA3 pyramidal cell and the resulting extracellular signal. The first negative extracellular peak corresponded to the maximal rate of rise of the action potential and the first positive peak to its peak. *C*, the amplitude of extracellular spikes, measured with the electrode at different distances from the recorded cell (20 distances, 10 pyramidal cells) diminished with increasing separation. It reached typical recording noise levels (dashed line at 15 μV) at a separation close to 80 μm. The fit assumes an inverse square relation between spike amplitude and distance. *D* shows the distance between the cell and the electrode estimated from the distance between the two planes of focus, with a correction for the approach angle of the electrode.

and at 8 mM K^+. The histogram obtained at 2 mM K^+ possesses several peaks. Spikes corresponding to the largest amplitude peak had a stereotyped form, suggesting that they derived from a single cell, while spikes corresponding to lower amplitude peaks were variable. In this experiment, increasing K^+ to 8 mM induced a sixfold increase in the frequency of detected spikes and peaks could no longer be resolved in the amplitude histogram (Fig. 3*C*). The distribution was fitted by a curve in which amplitude follows a power relation. The derivation is given in the Appendix.

When external K^+ was increased, stereotyped bursts of 3–8 extracellular spikes, with interspike intervals of 5–10 ms, became increasingly evident. These bursts might represent the activity of several cells or that of a single pyramidal cell firing complex spikes (Kandel & Spencer, 1961). In order to discriminate between these possibilities we attempted to identify activity generated by a single cell. Action potentials generated by one cell result in temporally coincident spikes when they are detected by multiple extracellular electrodes (McNaughton *et al.* 1983). Coincident spikes were frequently recorded when several tungsten electrodes (Fig. 4) were placed orthogonal to the CA3 stratum pyramidale – along the pyramidal cell somato-dendritic axis. When aquisition was triggered from the spikes recorded from stratum pyramidale, smaller coincident events could be detected up to 250 μm away from the cell body layer (Fig. 4*B*). Since correlated spikes were not recorded from electrodes separated by similar distances along stratum pyramidale, these coincident events probably reflect somatic and dendritic signals generated by the same cell. Furthermore, the form of somatic and dendritic events followed that expected for current sources and sinks (Nicholson & Freeman, 1975) associated with an active dendritic propagation of somatically generated action potentials (Spruston *et al.* 1995).

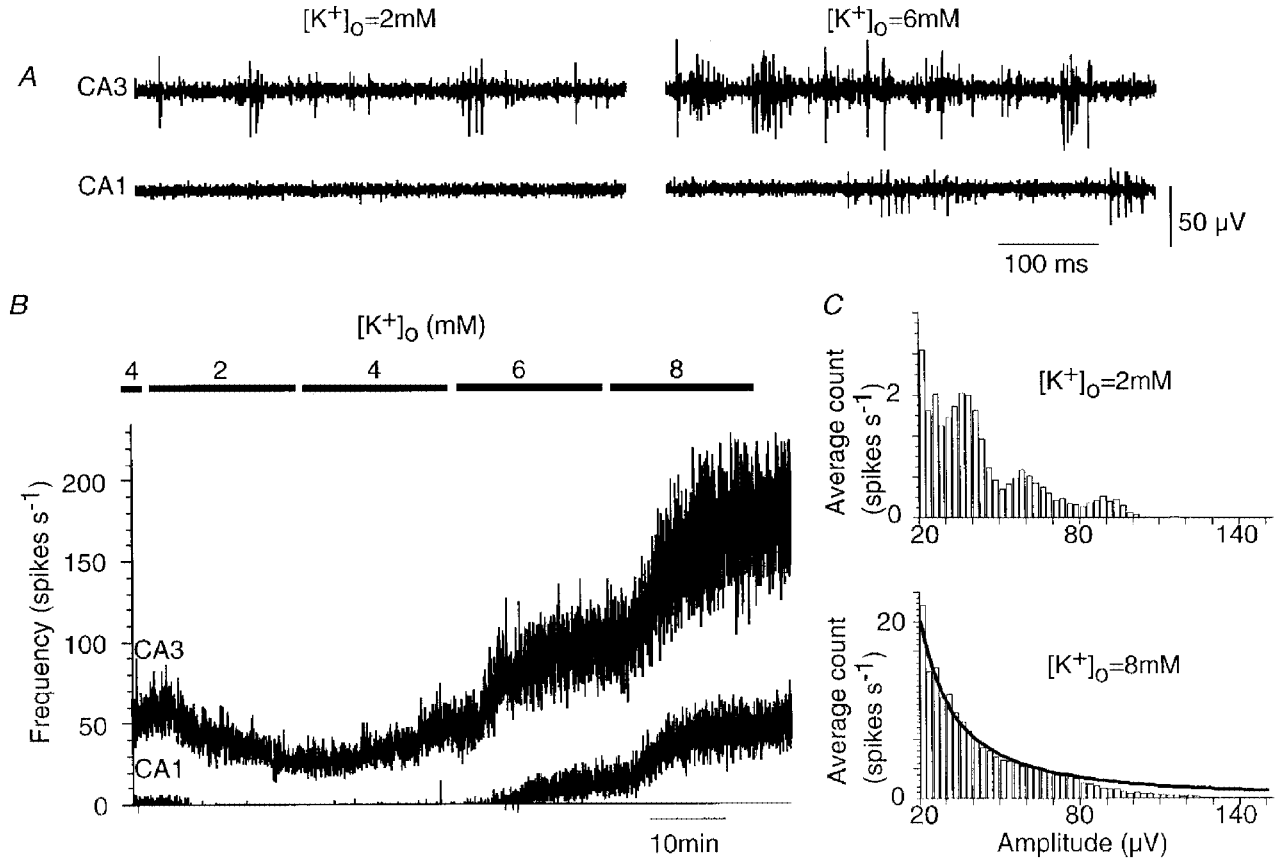

Figure 3. Effects of changes in K^+ on spontaneous activity of CA3 and CA1 cells

A, simultaneous records with one electrode located in CA3 and the other in CA1. Spikes were evident in the CA3 record at both 2 and 6 mM external K^+, while the record from the CA1 region was largely silent until K^+ was increased to 6 mM. *B*, changes in spike frequency measured from CA3 (upper trace) and from CA1 (lower trace) as K^+ was reduced from 4 to 2 mM and then increased to 8 mM in steps of 2 mM. *C*, histograms of spike amplitudes from the CA3 recording electrode in the presence of 2 and 8 mM K^+. At 2 mM K^+, peaks were apparent. At 8 mM K^+, the spike frequency was increased sixfold and the amplitude histogram was smooth. The amplitude distribution ($N(A)$) at 8 mM K^+ was fitted to an equation of the form, $N(A) = cA^{-b}$, assuming a uniform cell packing density and discharge frequency (see Appendix). The optimal fit was obtained with constants $b = 1{\cdot}505$ and $c = 990$, and the Kolmogorov-Smirnov test gave a value of $P = 0{\cdot}59$ (with $n = 3081$). The fit diverges from the observed distribution for spikes of large amplitude, corresponding to signals from cells close to the recording electrode.

Using records from several electrodes to identify the activity of a single cell, the timing, number of spikes and descending amplitude of spikes in a burst were consistently correlated in records from somatic and dendritic electrodes. Stereotyped bursts persisted in the presence of blockers of fast excitatory and inhibitory synaptic transmission (5 μM NBQX, 100 μM APV and 50 μM bicuculline), suggesting that they did not depend on synaptic inputs (Fig. 4*D*). However, reducing extracellular K^+ to levels below 3 mM abolished burst firing ($n = 6$ cells), suggesting that this discharge pattern depends on neuronal excitability (Fig. 4*D*).

How much activity is intrinsic – how much is synaptic?

In these *in vitro* conditions, the CA3 cell population generates spontaneous activity. We first used pharmacological tools to dissect the contributions of synaptic excitation and inhibition and the intrinsic properties of CA3 cells to these discharges. In 33 records from 11 slices, suppressing synaptic excitation with the antagonists NBQX (5 μM) and APV (100 μM) reduced the frequency of extracellular spikes to $77 \pm 35\%$ of control ($P < 0{\cdot}001$). Application of the $GABA_A$ receptor antagonist picrotoxin

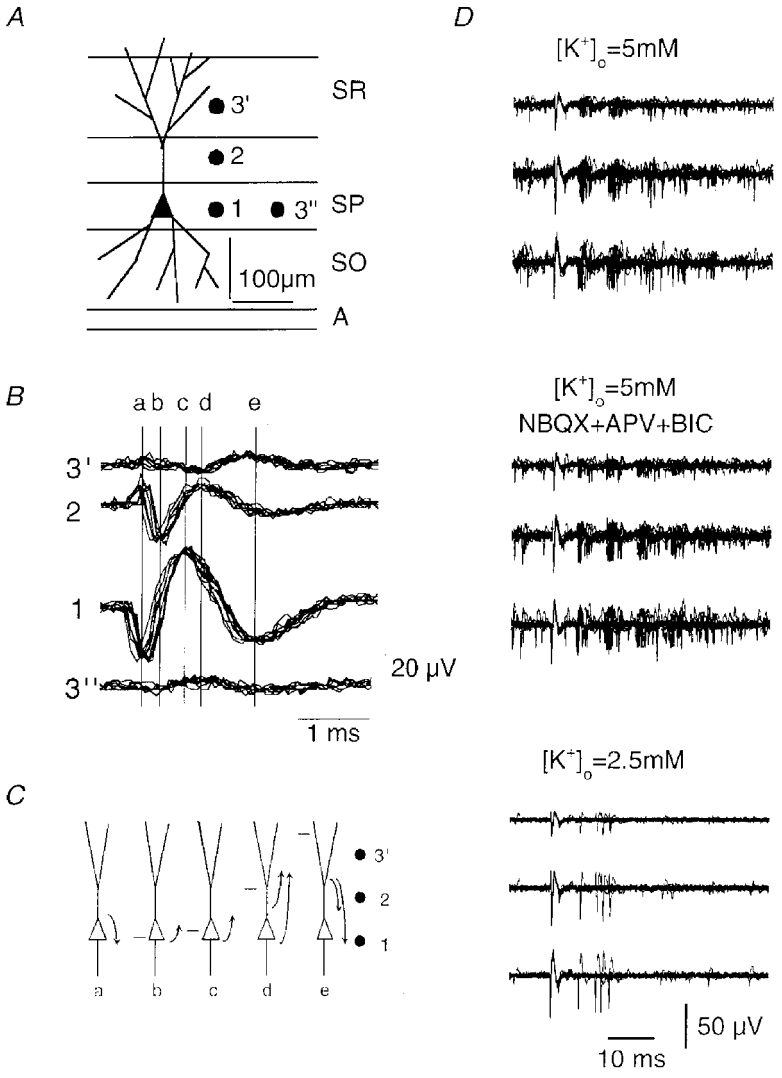

Figure 4. Recording of somatic and dendritic signals from the same pyramidal cell

A and *B*, records from three tungsten electrodes aligned orthogonally to the CA3 s. pyramidale (SP). Traces were triggered from the largest extracellular spike recorded from the electrode 1, located in SP. A correlated signal was recorded by electrode 2 (in s. lucidum, SL, at about 100 μm) and from electrode 3 (about 100 μm more distant in s. radiatum, SR). Trace 3″ shows the signal recorded on moving electrode 3 to a site in SP about 100 μm distant from electrode 1. *C*, the sequence of extracellular current fluxes at times *a*–*e* in *B* as deduced from the voltage difference between locations 1, 2 and 3′. The sequence corresponds to the initiation and back-propagation of an action potential with the site of maximum depolarisation indicated by a horizontal bar. *D*, triple records from three somato-dendritic sites, as in *A*, were used to follow the burst firing activity of a single CA3 cell (upper traces, $n = 10$ superimposed traces). Addition of 10 μM NBQX, 100 μM APV and 10 μM bicuculline (middle traces) did not suppress spontaneous burst firing, but bursts ceased when K^+ was reduced to 2·5 mM (lower traces).

(50 μM), in the presence of NBQX and APV, increased extracellular spike frquency to $177 \pm 71\%$ of its control value ($P < 10^{-9}$). Figure 5*A* shows changes in spike frequency recorded by one electrode during such an experiment and results from 33 records are summarised in Fig. 5*C*.

Intrinsic cellular properties seem likely to underly the spontaneous firing generated by CA3 cells when both fast synaptic excitation and synaptic inhibition were suppressed. Nonetheless, neurotransmitters such as glutamate and acetylcholine could be present in slices at levels that tonically excite CA3 cells. However, in seven slices tested, exposure to antagonists at metabotropic receptors for glutamate (MCPG, 200 μM) and muscarinic receptors (atropine, 10 μM) did not significantly alter the frequency of extracellular discharges.

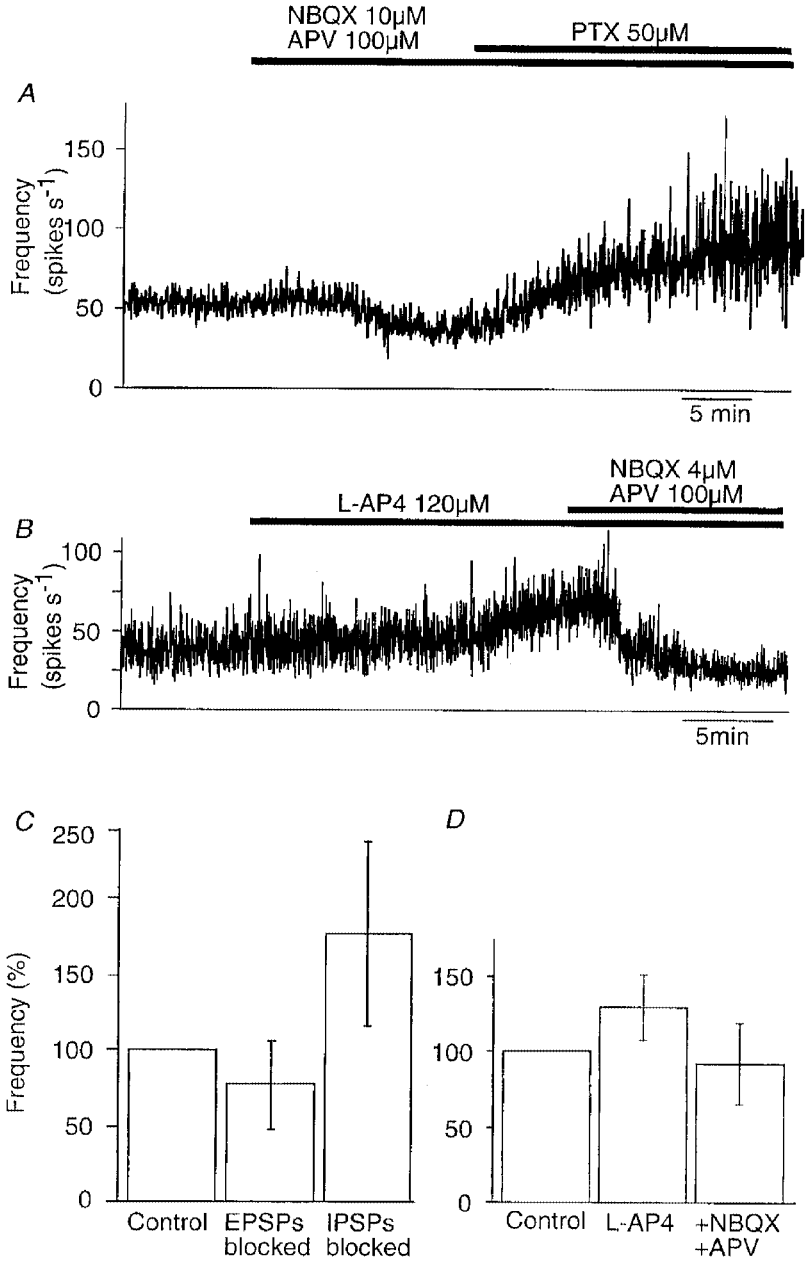

Figure 5. Effects on population activity of suppressing synaptic excitation and inhibition

A, the frequency of spontaneous activity recorded from the CA3 region derived from extracellular signals recorded in control solution, after the addition of 10 μM NBQX and 100 μM APV and then after the addition of 50 μM picrotoxin. *B*, the frequency of extracellular spikes recorded in control conditions, in the presence of 120 μM L-AP4 and after addition of 4 μM NBQX and 100 μM APV. *C*, summary of changes (mean $\pm$ S.D.) in firing frequency induced by application of blockers of excitatory amino acid receptors and then of GABA receptors ($n = 33$). *D*, summary of changes in activity induced by L-AP4 ($n = 23$) and subsequent blockade of excitatory amino acid receptors ($n = 20$).

The small effects of antagonists at excitatory amino acid receptors may suggest that synaptic excitation makes a minor contribution to CA3 cell activity. However, these antagonists will have blocked EPSPs impinging on both pyramidal cells and inhibitory cells. Suppressing EPSPs on inhibitory cells should tend to reduce inhibitory cell firing and so indirectly enhance pyramidal cell activity. One way to distinguish between the relative influences of synaptic excitation of CA3 pyramidal cells and interneurons on population firing might be to apply an agent that suppresses transmission at one or the other of these connections. Immunocytochemical (Shigemoto *et al.* 1997) and physiological (Scanziani *et al.* 1998) work suggests that type III metabotropic receptors for glutamate, which act to reduce transmitter release, are selectively expressed at excitatory synapses terminating on inhibitory but not pyramidal cells in the hippocampus. In 23 recordings, we found that application of an agonist of these receptors, L-AP4 (100–150 μM), increased activity to 133 ± 22% ($P < 0{\cdot}001$) of its control frequency (Fig. 5*B* and *D*). In 20 of these experiments, addition of the excitatory amino acid receptor antagonists NBQX (4 μM) and APV (100 μM) to an external solution that already contained L-AP4 reduced the frequency of extracellular spikes to 89 ± 26% of its control level. Although we cannot be sure that L-AP4 suppressed transmission completely and uniformly at all excitatory synapses terminating on inhibitory cells, our data suggest that this connection acts to reduce CA3 cell firing.

Contributions of intrinsic properties and synaptic events to spontaneous firing of CA3 pyramidal and inhibitory cells

Contributions of excitatory synaptic events to CA3 pyramidal and inhibitory cell firing were also compared by examining membrane potential trajectories immediately preceding action potentials. Spike initiation was studied in intracellular records from CA3 pyramidal cells ($n = 10$) that either discharged spontaneously ($n = 8$) or were made to fire at frequencies of 0·5–3 spikes s^{-1} ($n = 2$) by injecting small, maintained depolarising currents (Fig. 6*A*–*D*). Spontaneous EPSPs were apparent in all cells. Their amplitudes ranged from the lower limit of reliable detection, close to 0·3 mV, up to 1–2 mV (Miles & Wong, 1987). IPSPs of amplitude between 0·3 and 4 mV were also apparent in all records. Measurements from 350–500 action potentials suggested that EPSPs preceded 27 ± 6% (range 15–34%) of pyramidal cell action potentials (Fig. 6*B*). A higher proportion, 66–85% of action potentials, appeared to be initiated with no preceding EPSP (Fig. 6*C*). This may be an overestimate since small synaptic events probably escaped detection, but such EPSPs probably had smaller effects on spike timing. Synaptic inhibition may control pyramidal cell firing both by injecting a hyperpolarisation during the cycle of membrane repolarisation between action potentials (Fig. 6*A*) and also by suppressing or delaying spike initiation (Miles *et al.* 1996; Häusser & Clark, 1997). IPSPs occurred in the 50 ms preceding 12–26% of pyramidal cell action potentials (Fig. 6*D*).

The role of EPSPs in action potential initiation was also examined for ten inhibitory cells (Fig. 6*E*–*H*) recorded close to the stratum pyramidale in the CA3 region. These cells differed from pyramidal cells in that their action potentials were of shorter duration and were not followed by a depolarising after-potential and their membrane time constants were typically shorter. Eight of these cells discharged spontaneously. Spike initiation was examined in the absence of holding current or during the injection of small maintained currents to maintain a discharge frequency of 2–4 action potentials s^{-1}. In 8 out of 10 cells spontaneous hyperpolarising IPSPs were either absent or were rarely observed. In contrast, EPSPs were evident in all cells and preceded the majority of inhibitory cell action potentials (Fig. 6*F*). Measurements made from 250–400 action potentials showed that 86 ± 12% (range 68–99%) of spontaneous spikes were preceded by an EPSP of amplitude greater than 0·3 mV. The latency between EPSP onset and subsequent inhibitory cell firing ranged between 0·5 and 6 ms. The distribution of intervals between EPSP onset and action potential initiation is shown in Fig. 6*H*.

Effects of firing in single cells on extracellular activity

Since dentate granule cells were typically silent, most of the synaptic excitation that CA3 cells received in our slice preparations probably resulted from transmitter liberated by axon collateral synapses of other CA3 pyramidal cells (Miles & Wong, 1987; Ishizuka *et al.* 1990). Another way to examine the influence of synaptic excitation on firing in the CA3 cell population is therefore to measure how discharges in single pyramidal cells modify extracellular unit discharges (Fig. 7). Extracellular records were made with two or three tungsten electrodes located at distances of 200–800 μm from the intracellular electrode. In 31 of 205 simultaneous records, single pyramidal cell action potentials appeared to trigger extracellular spikes (Fig. 7*A*). These interactions were quantified by constructing spike-triggered averages of the instantaneous frequency of extracellular spikes. Such plots (Fig. 7*B*) show that intracellular action potentials were followed by a large increase in extracellular spike frequency. In this case, the latency to the increase in frequency was 1·5 ms and integration of the area under the peak suggested that about 40% of intracellular action potentials initiated an extracellular spike. A single peak was apparent in the amplitude histogram for spikes detected during this time window (Fig. 7*C*). A peak at the same amplitude in the distribution for spikes detected outside the time window suggested that the same unit also fired independently of action potentials in the recorded pyramidal cell. In 31 interactions (Fig. 7*D*), the mean latency between the intracellular action potential and extracellular spike onset was $2{\cdot}2 \pm 1{\cdot}0$ ms and the mean probability that a spike was triggered was $0{\cdot}36 \pm 0{\cdot}16$ ($n = 31$). In 19 interactions, the amplitude and form of triggered spikes were similar, suggesting that they were

generated by a single cell. In the other 12 records, it was difficult to be certain that a single spike was initiated and often at least two units with distinct forms were apparent.

Burst firing in single pyramidal cells seems likely to have stronger effects on population activity, than single action potentials. In 36 out of 195 simultaneous records, intracellular bursts initiated an increase in the summed frequency of extracellular spikes (Fig. 8). Typically an increase occurred at short latencies after the first spike of the burst (Fig. 8*A*) but two qualitatively different responses

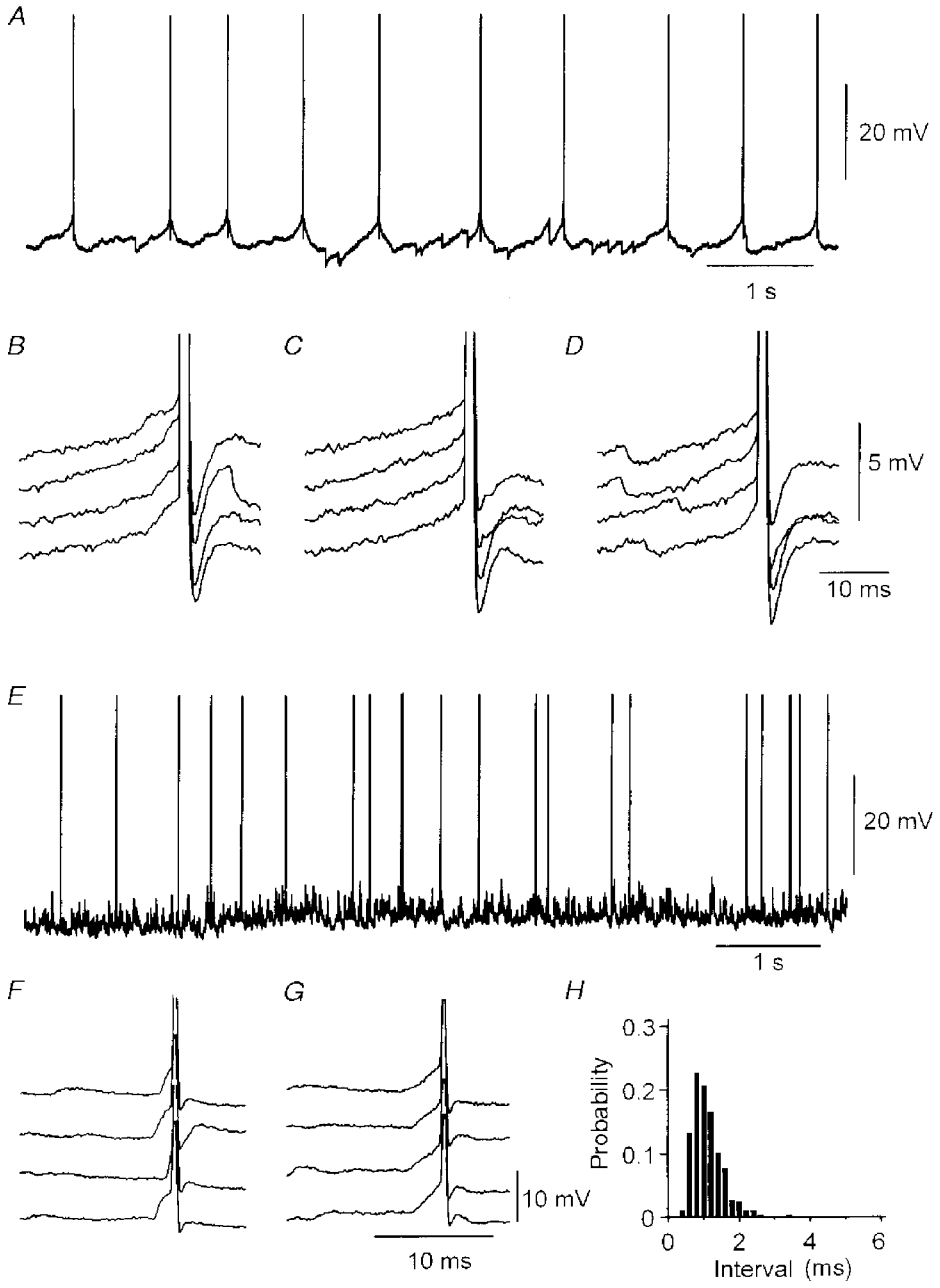

Figure 6. Spontaneous synaptic events and CA3 cell firing

A, spontaneous discharge of a CA3 pyramidal cell (spikes are cut) with no injected current. Hyperpolarisations due to IPSPs impinging during the repolarisation trajectory between spikes appear to increase the interval between action potentials. *B*, in this cell 28% of action potentials ($n = 529$) were preceded by an EPSP. *C*, 72% of action potentials appeared to be initiated in the absence of an EPSP (larger than 0·3 mV). *D*, an IPSP occurred in the 20 ms preceding the generation of 22% of action potentials. *E*, the spontaneous discharge of a CA3 inhibitory cell (spikes are cut) with no injected current. *F* and *G*, in this cell 95% of action potentials ($n = 450$) were preceded by an EPSP (*F*), while 5% of the action potentials appeared to be initiated in the absence of an EPSP (*G*). Spontaneous, hyperpolarising IPSPs were difficult to detect at resting potential in this cell. *H*, histogram of intervals between EPSP onset and action potential initiation ($n = 450$).

were also observed. In eight records, the increase in frequency followed only the second and subsequent spikes of the burst (Fig. 8*C*; cf. Fig. 12 of Ali & Thomson, 1998). Inhibitory effects on population discharges were much more common ($n = 25$) in responses to burst discharges than to single pyramidal cell spikes. Burst-triggered averages revealed a decrease, typically of 50–150 ms duration, in the frequency of extracellular firing. Decreases could occur in isolation but more often followed an initial increase in frequency of extracellular unit discharges (Fig. 8*B*).

Correlation of extracellular spikes with intracellular synaptic events

It is difficult to attribute extracellular unit activity, such as that shown in Figs 7 and 8, to firing of a pyramidal or an inhibitory cell. One way to identify a unit as excitatory or inhibitory is to correlate its occurrence with synaptic events in intracellular records. In most extracellular records, two or three large spikes could be reliably distinguished by their amplitude and form (Fig. 9*A* and *B*). In 13 of 205 simultaneous records, an identified extracellular spike consistently preceded an intracellular IPSP (Fig. 9*A* and *C*). These interactions were presumed to be monosynaptic since there were no or very few failures (3 ± 3% failures) and the mean IPSP latency was $0{\cdot}9 \pm 0{\cdot}2$ ms ($n = 13$). The mean IPSP amplitude was $1{\cdot}8 \pm 1{\cdot}0$ mV. We could not, in many recordings, detect an extracellular spike that consistently preceded intracellular EPSPs in a CA3 pyramidal cell.

Pyramidal cells cause spontaneously active inhibitory cells to fire at short latency

Identifying extracellular spikes as inhibitory by their relation to intracellular IPSPs allowed us to identify some units discharged by single pyramidal cell spikes. In five such

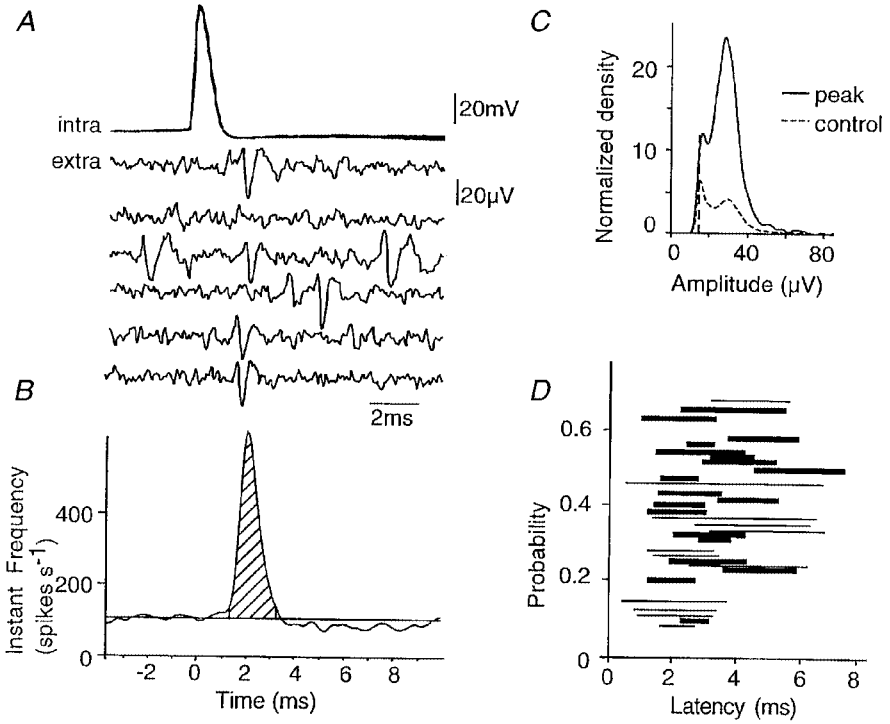

Figure 7. Single pyramidal cell action potentials initiate extracellular unit firing

A, six superimposed action potentials from a CA3 pyramidal cell together with corresponding traces from an extracellular electrode. A unit discharge occurs with latency 2–3 ms in four of the extracellular records. *B*, instantaneous frequency of extracellular firing, triggered from intracellular action potentials ($n = 2600$ sweeps). A peak was apparent in the instantaneous frequency function between latencies from the intracellular action potential of $1{\cdot}2$ and $3{\cdot}2$ ms (measured at 5% of the increase in frequency). The integral of this peak (hatched; see Methods) gives the probability that a single intracellular action potential initiated additional unit spikes. The probability in this case was $0{\cdot}43$. *C*, amplitude distribution (cf. Fig. 3*C*) for all unit spikes detected during the recording (control, dashed line) and for those ocurring during the peak of increased instantaneous frequency (peak, continuous line). An extracellular event of amplitude 30–40 μV was evident in both the peak and the control histogram, suggesting that the unit activated by intracellular action potentials discharged spontaneously during control periods. Note that the area under the histogram corresponding to the peak is larger than that under the control histogram, since the discharge frequency was higher during the period of the peak. *D*, plot of the probability that a unit spike was initiated against its latency for 31 interactions. The probability was estimated as in *B* and the latency is that between 5 and 95% of the increase in extracellular activity. Thin lines represent interactions where inspection of individual traces and of the amplitude distribution histogram suggested that discharge of a single unit was initiated, while thick lines are used for interactions where several distinct units appeared to discharge.

simultaneous records, pyramidal cell action potentials initiated extracellular spikes at short latency, while reciprocally the extracellular spike consistently preceded an intracellular IPSP (Fig. 10). Such interactions were maintained in the presence of elevated concentrations of divalent cations (4 mM Ca^{2+} and 4 mM Mg^{2+}), providing further evidence for monosynaptic coupling. In these conditions the frequency of spontaneous extracellular spikes was greatly reduced but the identified inhibitory units continued to discharge spontaneously. In these reciprocal interactions, pyramidal cell excitation discharged inhibitory cells by efficiently resetting their spontaneous activity.

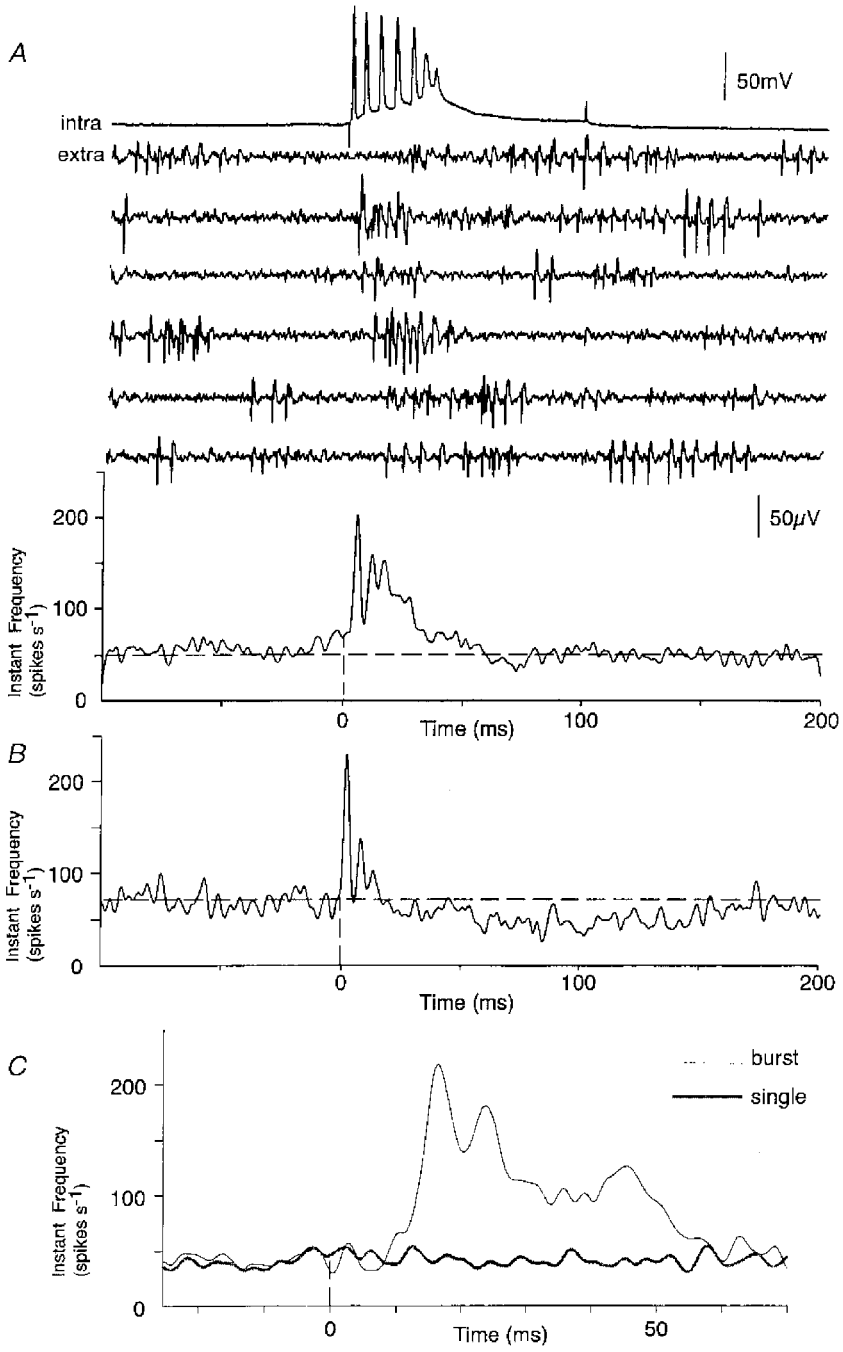

Figure 8. Effect of pyramidal cell burst firing on extracellular activity

A, simultaneous record of intracellular burst discharges elicited by current injection (top trace) and extracellular traces (middle six traces). The averaged instantaneous frequency (lower trace, $n = 650$ bursts), aligned with the first intracellular action potential showed a large increase in extracellular activity. *B*, in a different interaction pyramidal cell, bursts induced an initial increase in activity, of latency 3 ms and duration 20 ms, followed by a reduction in activity of duration about 180 ms. *C*, averaged instantaneous frequency plots from an interaction in which single pyramidal cell action potentials had no effect on population activity, but bursts induced an increase in extracellular firing after the second intracellular spike.

Direct evidence for the influence of inhibitory cell firing on population activity was obtained in simultaneous extracellular and intracellular records from inhibitory cells. In the traces shown in Fig. 11, spontaneously occurring inhibitory cell action potentials preceded a significant reduction in ensemble activity from a local extracellular electrode (Fig. 11*A* and *B*). Reductions in the frequency of extracellular firing were initiated by 7 out of 15 inhibitory cells examined (9 of 33 intracellular–extracellular interactions). The time course of these reductions resembled that of an intracellular IPSP, with a rapid onset and a slower decaying phase of duration several tens of milliseconds.

Intracellular records from inhibitory cells, togther with extracellular measurements of population activity, provided further evidence that the synapses which excite inhibitory cells are functionally highly effective. For the interaction shown in Fig. 11, spontaneously occurring inhibitory cell action potentials were preceded by a large increase in the instantaneous frequency of extracellular activity (Fig. 11*C* and *D*). A similar increase in extracellular spike frequency occurred in 10 of 33 records from interneurons. Extracellular spikes often appeared to be correlated with the onset of inhibitory cell EPSPs in the inhibitory cell, and their form and amplitude was typically variable, suggesting that multiple presynaptic cells were involved.

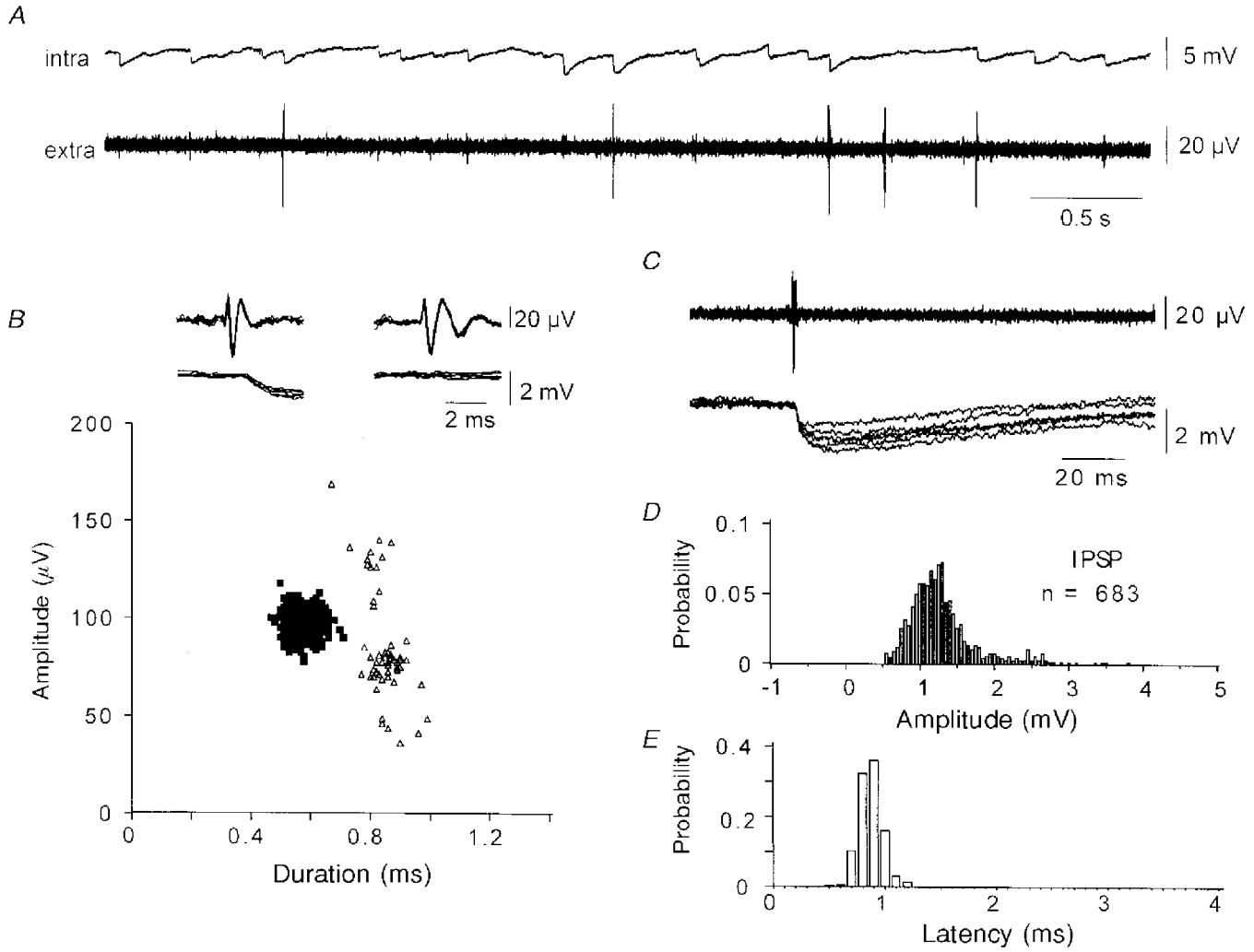

Figure 9. Extracellular spikes trigger intracellular IPSPs

A, simultaneous pyramidal cell and extracellular records made in the presence of elevated divalent cations (Ca^{2+} and Mg^{2+}, 4 mM). Some of the largest amplitude extracellular spikes appeared to precede intracellular IPSPs. *B*, extracellular spikes ($n = 754$) were sorted by amplitude and by time between the two positive spike maxima. Spikes corresponding to the cluster of amplitude about 100 μV and duration about 0·6 ms invariably preceded IPSPs (■). In contrast spikes of similar amplitude but duration about 0·8 ms were not associated with intracellular IPSPs (△). *C*, short-duration extracellular spikes preceded intracellular IPSPs. *D*, amplitude histogram for IPSPs following 683 short duration spikes. IPSP amplitude was measured between a time preceding the unit spike and a time equal to the peak of an averaged event. Note the absence of IPSP failures. *E*, histogram of latencies between the onset of the unit spike and that of the IPSP. The mean latency was 0·88 ± 0·32 ms ($n = 683$).

Synaptic excitation becomes more effective when synaptic inhibition is reduced

We wished to test whether excitatory synapses between CA3 cells contribute more effectively to the generation of population activity when the efficacy of synaptic inhibition is reduced. However, a complete block of $GABA_A$ receptors generates synchronous epileptiform discharges during which the effects of a single cell on the surrounding cell population are difficult to determine. We found that concentrations of bicuculline between 0·5 and 2·5 μM increased the frequency of extracellular spikes to 161 ± 37% ($n = 39$, $P < 10^{-9}$) of its control value, without initiating fully synchronous discharges (Fig. 12). Application of the excitatory amino acid receptor antagonists NBQX (5 μM) and APV (100 μM) to slices where inhibition was already partially suppressed, reduced the frequency of extracellular spikes to 83 ± 22 ($n = 39$, $P < 0{\cdot}001$) of control (Fig. 12). Thus suppressing excitation with synaptic inhibition already partially suppressed reduced activity by 48%, whereas suppressing excitation with inhibition active caused a reduction of only 23% (cf. Fig. 5).

In 65 paired intra- and extracellular recordings we compared the effect of a pyramidal cell burst on population activity before and after partial suppression of synaptic inhibition. In control conditions, four types of response were observed – no effect, an increase, a decrease, or an increase succeeded by a decrease. In twelve recordings responses were modified after application of bicuculline (1·5–3 μM). A cell that previously had no effect on population activity initiated an increase in the presence of bicuculline in five records (Fig. 12*C*). In four records a decrease in population activity was abolished (Fig. 12*D*), and in three records an increase in extracellular activity was enhanced. These data suggest that excitatory pathways become more effective as the efficacy of transmission in inhibitory circuits is reduced.

DISCUSSION

This study aimed to characterise intrinsic and synaptic contributions to spontaneously occurring neuronal discharges in the CA3 region of hippocampal slices. We find

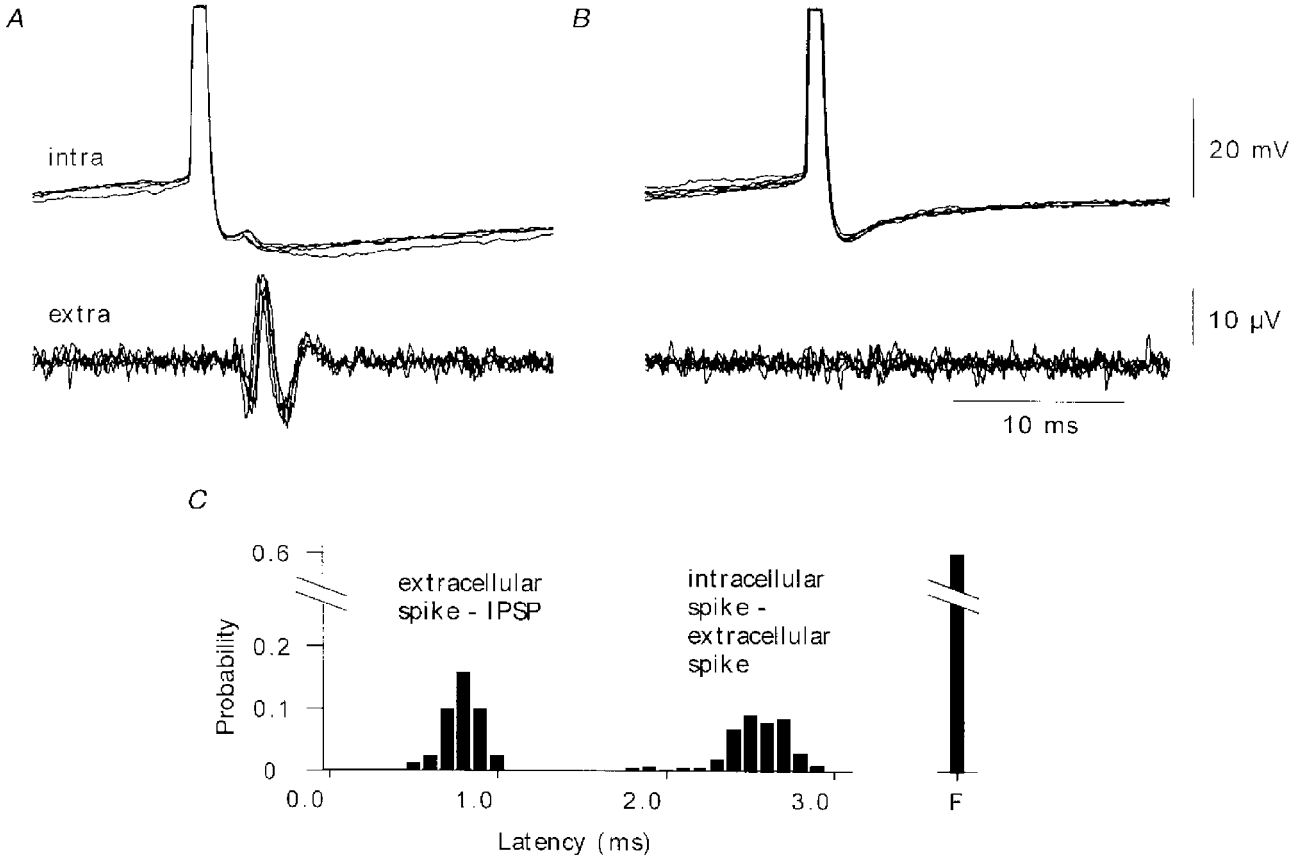

Figure 10. The extracellular spikes activated by pyramidal cell firing are generated by interneurons
Simultaneous pyramidal cell and extracellular record made in the presence of 4 mM Ca^{2+} and 4 mM Mg^{2+}. *A*, some intracellular action potentials, initiated by current injection, were succeeded by extracellular spikes ($n = 169$ of 428). Extracellular spikes preceded an IPSP in the pyramidal cell (six superimposed traces) *B*, IPSPs were not initiated when the unit spike did not occur. *C*, distributions of intervals between onset of the pyramidal cell action potential and the unit spike (intracellular–extracellular mean latency 2·4 ± 0·2 ms) and between the extracellular spike and the onset of the IPSP (extracellular–IPSP mean latency 0·7 ± 0·1 ms). 'F' corresponds to failures.

that, *in vitro*, CA3 population activity originates largely in the intrinsic cellular properties of pyramidal cells (Figs 5 and 6). Synaptic inhibition acts to restrain the spontaneous activity of CA3 cells (Fig. 5). The effect of synaptic excitation on CA3 population activity is more complex since two types of excitatory synapse with opposing actions on ensemble firing are involved – those by which pyramidal cells excite other pyramidal cells and those that excite inhibitory cells. Our data suggest that excitatory synapses terminating on inhibitory cells are more effective in transmitting firing than those that excite pyramidal cells (Figs 5, 6, 10 and 11).

Considerations on the method

Simultaneous whole cell and extracellular records suggest that tungsten electrodes detect spikes generated by cells located at distances of up to 80 μm (Fig. 2). Dual extracellular recordings (Fig. 4*B*) provide additional evidence that 80 μm is an approximate spatial limit on the detection of activity. This suggests that the electrodes used in this study may have recorded activity from 400–500 CA3 pyramidal cells. The use of extracellularly recorded action potentials from a cluster of several hundred cells as an index of population activity has advantages and disadvantages. It is a non-invasive method that does not compromise action potential generation in recorded cells. Spike frequency summed over a population of several hundred neurons is a more sensitive measure of population activity than extracellular field potentials. However, signals recorded from the CA3 stratum pyramidale are clearly mixed in that they include spikes generated by both inhibitory and pyramidal cells. Furthermore, since signals from multiple cells are recorded simultaneously, spikes generated by different cells may superimpose at high frequencies.

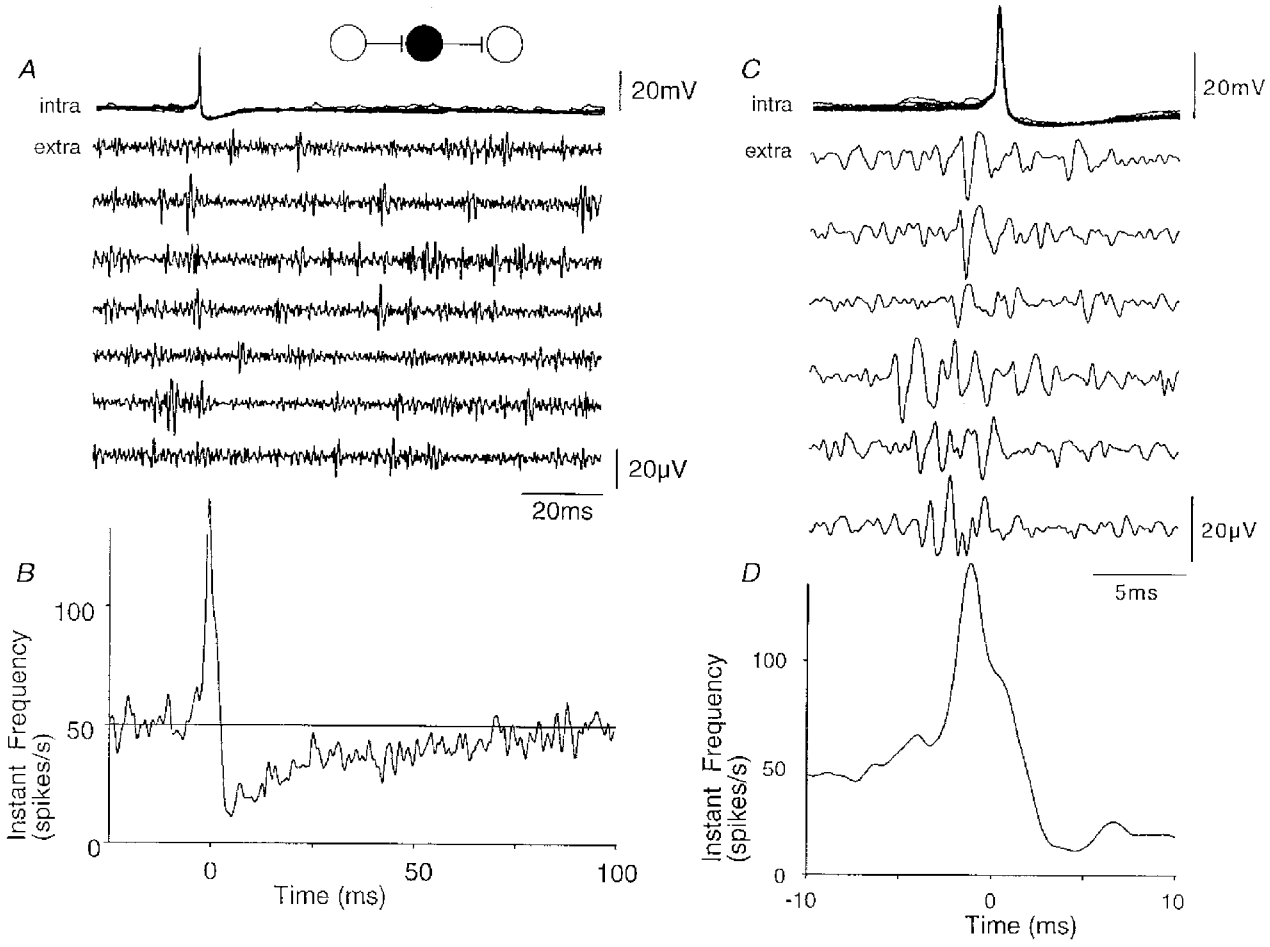

Figure 11. Correlations between inhibitory cell firing and population activity

A, ten superimposed action potentials from a spontaneously active CA3 inhibitory cell and simultaneous extracellular records. Unit activity is reduced following the intracellular action potential. *B*, instantaneous frequency of extracellular activity triggered with respect to the intracellular spike (time $t = 0$; $n = 1600$ sweeps). Population activity was reduced to a minimum of about 30 % of its control level at about 4 ms after the inhibitory cell spike, and returned to control with time constant near 30 ms. The frequency of extracellular activity reached a peak before the inhibitory cell action potential. *C*, extracellular events, probably deriving from several distinct units, preceded inhibitory cell firing. *D*, the instantaneous frequency function shows that the increase in extracellular activity started at about 6 ms before and reached a peak at 2 ms before inhibitory cell action potentials.

Spontaneous ensemble activity in the hippocampal slice

There were clear differences in the resting activity of different cell types in our experimental conditions. CA3 pyramidal cells discharged spontaneously, while CA1 pyramidal cells were largely silent (Fig. 3). Some inhibitory cells seem to be more excitable than pyramidal cells (Fricker *et al.* 1999). Presumably different conductances control resting potential and determine firing threshold in these different cell types. Spontaneous population activity recorded from single sites in the CA3 region was typically tonic with small variations in instantaneous frequency except for the bursts of action potentials generated by single CA3 pyramidal cells (Fig. 4).

Contributions of intrinsic activity of CA3 pyramidal cells to spontaneous ensemble activity

Our data suggest that population activity recorded from the CA3 region depends strongly on non-synaptically driven, spontaneous pyramidal cell firing. Blocking receptors activated by both excitatory and inhibitory amino acid transmitters increased the frequency of extracellular discharges by about 80% (Fig. 5). Furthermore, when fast synaptic excitation was functional, a high proportion of action potentials discharged by CA3 pyramidal cells appeared to occur independently of excitatory synaptic events (see Fig. 6). This is consistent with reports that some neurons possess an auto-activity when isolated from all synaptic inputs (Alving, 1968; Kay & Wong, 1986; Feigenspan *et al.* 1998). However, neuronal excitability seems likely to vary within the CA3 pyramidal cell population since increasing extracellular K^+ recruited previously silent cells to discharge (Fig. 3).

Effects of synaptic inhibition on spontaneous ensemble activity

Synaptic inhibition exerts a strong braking effect on spontaneous activity in the CA3 region. When synaptic

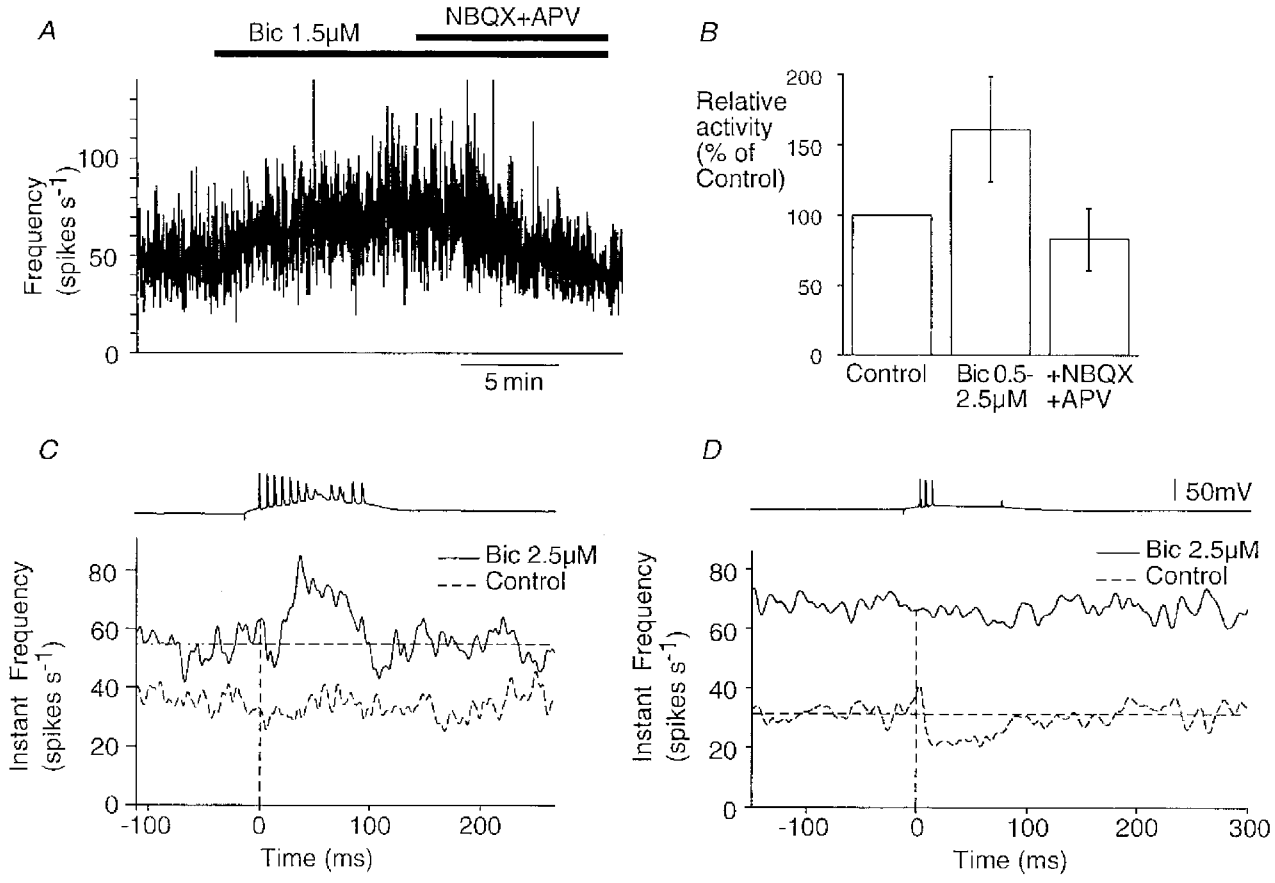

Figure 12. Partial block of synaptic inhibition modifies the effect of pyramidal cell firing on population activity

A, modifications in extracellular spike frequency induced by perfusion of 1·5 μM bicuculline (Bic) followed by addition of NBQX (4 μM) and APV (100 μM). *B*, summary of changes in activity ($n = 39$). *C* and *D*, comparison of the effects of a pyramidal cell bursts on ensemble activity before and after bicuculline application. In each case, the upper trace shows an intracellular burst, and lower traces are extracellular records; in the instantaneous frequency plots the control effect on extracellular activity is shown by a dashed line and the bicuculline effect by a continuous line. Bicuculline could reveal an excitatory action on population activity of burst firing in a cell that previously had no effect (*C*), or suppressed an inhibitory effect of pyramidal cell burst firing (*D*), on population activity.

excitation was already suppressed, suppressing IPSPs mediated by $GABA_A$ receptors increased firing frequency by about 80% over its control value (Fig. 5). Furthermore activation of some individual inhibitory cells initiated a strong reduction in population firing with a time course similar to that of intracellular IPSPs (Fig. 11; cf. Brink *et al.* 1983). It would be interesting to correlate the location of axon terminals established by an inhibitory cell with the efficacy of its actions on population activity. The inhibitory cells recorded in this study, located near stratum pyramidale, tend to form synapses with pyramidal cell somata, and thus may exert a stronger control over population firing than do inhibitory cells which synapse with pyramidal cell dendrites (Eccles, 1969; Miles *et al.* 1996; Häusser & Clark, 1997).

Effects of synaptic excitation of inhibitory cells in controlling ensemble activity

Several approaches suggest that excitatory synapses terminating on inhibitory cells contribute to a strong feedback inhibition of CA3 cell population activity. L-AP4 application increased the frequency of extracellular unit activity (Fig. 5*B* and *D*), presumably via a presynaptic reduction in efficacy at excitatory synapses terminating on inhibitory cells (Shigemoto *et al.* 1997; Scanziani *et al.* 1998). Examination of action potential initiation in inhibitory cells also suggested that this synapse has strong functional effects. A high proportion of inhibitory cell action potentials appeared to be initiated by EPSPs, in sharp contrast to the situation in pyramidal cells (Figs 6 and 11). This difference may imply that the inhibitory cells we recorded, close to s. pyramidale, may correspond more closely to the ideal of a neuron as a coincidence detector (König *et al.* 1996) than do CA3 pyramidal cells.

The effects of activity in single pyramidal cells on extracellular population discharges (Fig. 7) provided further evidence that synaptic excitation of CA3 inhibitory cells is functionally strong. Unit spikes could be discharged at latencies of 2–6 ms and with probabilities as high as 0·7. The extracellular spike could, in some cases, be identified as being generated by an inhibitory cell by showing that it initiated, reciprocally, an IPSP in the recorded pyramidal cell (Fig. 10). Comparison with dual intracellular records (Miles, 1990) and with recent *in vivo* work (Csicsvari *et al.* 1998) suggests that many, if not all, extracellular units that were discharged by single pyramidal cell spikes may have been generated by inhibitory cells. Extracellular, and so non-invasive recordings, reinforce the suggestion that a unitary EPSP can discharge an inhibitory cell (Miles, 1990; Barbour, 1993; Csicsvari *et al.* 1998) and reveal that postsynaptic cells may be autonomously active. Pyramidal cell excitation of peri-somatic inhibitory cells may function to reset the timing of their spontaneous firing (Reyes & Fetz, 1993) rather than to depolarize silent cells to firing threshold. Excitatory synaptic events impinging on inhibitory cells have a rapid time course (Geiger *et al.* 1997) which may act to facilitate this resetting (Mainen & Sejnowski, 1995).

Contribution to population activity of excitatory synapses terminating on pyramidal cells

In the absence of granule cell activity, recurrent excitatory synapses established by CA3 pyramidal cells represent the major source of synaptic excitation in the CA3 region. Our data suggest that EPSPs mediated by these synapses enhanced pyramidal cell firing to a small extent when synaptic inhibition was functional. A minority (20–40%) of pyramidal cell action potentials appeared to be triggered by EPSPs (Fig. 6). Further, in dual records we did not detect extracellular spikes that consistently preceded intracellularly recorded EPSPs. However, the contribution of recurrent excitation to population discharges was increased when the efficacy of inhibitory circuits was reduced either by partially suppressing $GABA_A$ receptor-mediated IPSPs (Fig. 12) or by suppressing excitatory inputs to inhibitory cells with L-AP4 (Fig. 5*B*). It is interesting that during behavioural states associated with learning in the intact animal, inhibitory cell firing is reduced (Wilson & McNaughton, 1993), thus presumably permitting a more effective communication between pyramidal cells.

APPENDIX

The distribution of spike amplitudes recorded by an extracellular electrode depends on the spatial distribution of cells around the electrode and their firing activity. To derive this relation, for a given cell we define A as the amplitude of the spike and r as the distance from electrode. The distribution, $N(A)$, corresponding to the amplitude histogram is:

$$N(A) = \mathrm{d}n/\mathrm{d}A,$$

where $\mathrm{d}n$ is the number of spikes of amplitudes between A and $\mathrm{d}A$. These spikes originate from cells located between r and $r + \mathrm{d}r$ on both sides of the electrode along the stratum pyramidale. If we assume that both cells and their firing frequencies are homogeneously distributed, this equation becomes:

$$\mathrm{d}n = N(A)\mathrm{d}A = 2\lambda\mu(-\mathrm{d}r),$$

where λ is the density of cells along s. pyramidale and μ is the number of spikes that a cell discharges during the period considered. Therefore the amplitude distribution becomes:

$$N(A) = -2\lambda\mu(\mathrm{d}r/\mathrm{d}A).$$

A physiologically precise model (Clark & Plonsey, 1968) has shown that, at very short distances, the relation between extracellular spike amplitude and distance does not follow a simple power law, since axial currents cannot be neglected. However, at longer distances, for pyramidal cells the relation becomes:

$$A = c/r^{\alpha},$$

where c is a constant and α an exponent related to the dimensionality of extracellular space. And the spike amplitude distribution becomes:

$$N(A) = \frac{2\lambda\mu c^{1/\alpha}}{\alpha A^{(1/\alpha)+1}} = \frac{c'}{A^{(1/\alpha)+1}},$$

where c' is a compound constant. At all but small distances, the model of Clark and Plonsey was fitted by $\alpha = 2$, which is the value that we used for the graph shown in Fig. 2*C*. For $\alpha = 2$, the spike amplitude distribution should follow the form $N(A) = c'A^{-1.5}$, which is close to our experimental observation (Fig. 3*C*).

Ali, A. B. & Thomson, A. (1998). Facilitating pyramid to horizontal oriens-alveus interneurone inputs: dual intracellular recordings in slices of rat hippocampus. *Journal of Physiology* **507**, 185–199.

Alving, B. O. (1968). Spontaneous activity in isolated somata of *Aplysia* pacemaker neurons. *Journal of General Physiology* **51**, 21–45.

Baldwin, H. A., Frank, S. & Lettvin, J. Y. (1965). Glass coated tungsten microelectrodes *Science* **148**, 1462–1464.

Barbour, B. (1993). Synaptic currents evoked in Purkinje cells by stimulating individual granule cells. *Neuron* **11**, 759–769.

Brink, E., Harrison, P. J., Jankowska, E., McCrea, D. A. & Skoog, B. (1983). Post-synaptic potentials in a population of motoneurones following activity of single interneurones in the cat. *Journal of Physiology* **341**, 341–359.

Buhl, E. H., Hálásy, K. & Somogyi, P. (1994). Diverse sources of hippocampal unitary inhibitory postsynaptic potentials and the number of synaptic release sites. *Nature* **368**, 823–828.

Buzsáki, G. (1984). Long term changes of hippocampal sharp waves following high frequency afferent stimulation. *Brain Research* **300**, 179–182.

Churchland, P. S. & Sejnowski, T. J. (1988). Perspectives on cognitive neuroscience. *Science* **262**, 741–745.

Clark, J. & Plonsey, R. (1968). The extracellular potential field of the single active nerve fiber in a volume conductor. *Biophysical Journal* **8**, 842–864.

Csicsvari, J., Hirase, H., Csurko, A. & Buzsáki, G. (1998). Reliability and state dependence of pyramidal cell – interneuron synapses in the hippocampus: an ensemble approach in the behaving rat. *Neuron* **21**, 179–189.

Eccles, J. C. (1969). *The Inhibitory Pathways of the Central Nervous System*, pp. 101–105. Liverpool University Press, Liverpool, UK.

Feigenspan, A., Gustincich, S., Bean, B. P. & Raviola, E. (1998). Spontaneous activity of solitary dopaminergic cells of the retina. *Journal of Neuroscience* **18**, 6776–6789.

Fricker, D., Verheugen, J. A. H. & Miles, R. (1999). Cell-attached measurements of the firing threshold of hippocampal neurones. *Journal of Physiology* **517**, 791–804.

Geiger, J. R., Lübke, J., Roth, A., Frotscher, M. & Jonas, P. (1997). Submillisecond AMPA receptor mediated signalling at a principal neuron – interneuron synapse. *Neuron* **18**, 1009–1023.

Gulyás, A. I., Miles, R., Sik, A., Tòth, K., Tamamaki, N. & Freund, T. F. (1993). Hippocampal pyramidal cells excite inhibitory neurons via a single release site. *Nature* **366**, 683–687.

Häusser, M. & Clark, B. A. (1997). Tonic synaptic inhibition modulates neuronal output pattern and spatiotemporal synaptic integration. *Neuron* **19**, 665–678.

Hubbard, J. I., Llinas, R. & Quastel, D. M. J. (1969). *Electrophysiological Analysis of Synaptic Transmission*. Williams & Wilkins, Baltimore.

Hubel, H. D. (1957). Tungsten micro-electrodes for recording from single cells. *Science* **125**, 549–550.

Ishizuka, N., Weber, J. & Amaral, D. G. (1990). Organisation of intrahippocampal projections originating from CA3 pyramidal cells in the rat. *Journal of Comparative Neurology* **295**, 580–623.

Kandel, E. R. & Spencer, W. A. (1961). Electrophysiology of hippocampal neurons. II. Afterpotential and repetitive firing. *Journal of Neurophysiology* **24**, 243–259.

Kay, A. R. & Wong, R. K. S. (1986). Isolation of neurons suitable for patch clamping from adult mammalian central nervous system. *Journal of Neuroscience Methods* **16**, 227–238.

Kim, U., Bal, T. & McCormick, D. A. (1995). Spindle waves are propagating synchronised oscillations in the ferret LGNd *in vitro*. *Journal of Neurophysiology* **74**, 1301–1323.

König, P., Engel, A. K. & Singer, W. (1996). Integrator or coincidence detector? The role of the cortical neuron revisited. *Trends in Neurosciences* **19**, 130–137.

Lorente de Nò, R. (1947). *A Study of Nerve Physiology*. Rockefeller Institute Monograph No. 132, chap. XVI. Rockefeller Institute, New York.

McNaughton, B. L., O'Keefe, J. & Barnes, C. A. (1983). The stereotrode: a new technique for simultaneous isolation of several single units in the central nervous system from multiple unit records. *Journal of Neuroscience Methods* **8**, 391–397.

Mainen, Z. F. & Sejnowski, T. J. (1995). Reliability of spike timing in neocortical neurons. *Science* **268**, 1503–1506.

Markram, H., Lübke, J., Frotscher, M., Roth, A. & Sakmann, B. (1997). Physiology and anatomy of synaptic connections between thick tufted pyramidal neurones in the developing rat neocortex. *Journal of Physiology* **500**, 409–440.

Meister, M., Wong, R. O., Baylor, D. & Shatz, C. J. (1991). Synchronous bursts of action potentials in ganglion cells of the developing mammalian retina. *Science* **252**, 939–943.

Miles, R. (1990). Excitation of inhibitory cells by single CA3 pyramidal cells in the guinea-pig hippocampus *in vitro*. *Journal of Physiology* **428**, 61–77.

Miles, R. & Poncer, J.-C. (1996). Paired recordings from neurons. *Current Opinion in Neurobiology* **6**, 387–394.

Miles, R., Tòth, K., Gulyás, A. I., Hájos, N. & Freund, T. F. (1996). Differences between dendritic and somatic inhibition in the hippocampus. *Neuron* **16**, 815–825.

Miles, R. & Wong, R. K. S. (1987). Inhibitory control of local excitatory circuits in the guinea-pig hippocampus. *Journal of Physiology* **388**, 611–629.

Mintz, I. M. & Korn, H. (1991). Serotonergic facilitation of quantal release at central inhibitory synapses. *Journal of Neuroscience* **11**, 3359–3370.

Nelson, D. A. & Katz, L. C. (1995). Emergence of functional circuits in ferret visual cortex visualised by optical imaging. *Neuron* **15**, 23–34.

Nicholson, C. & Freeman, J. A. (1975). Theory of current source density analysis and determination of conductivity tensor for anuran cerebellum. *Journal of Neurophysiology* **38**, 356–368.

Prince, D. A. & Tseng, G. F. (1993). Epileptogenesis in chronically injured cortex: *in vitro* studies. *Journal of Neurophysiology* **69**, 1276–1291.

Reyes, A. D. & Fetz, E. E. (1993). Two modes of interspike interval shortening by brief transient depolarisations in cat neocortical neurons. *Journal of Neurophysiology* **69**, 1661–1672.

Sanderson, A. C. & Kobler, B. (1976). Sequential interval analysis of non-stationary neuronal spike trains. *Biological Cybernetics* **22**, 61–67.

Scanziani, M., Gähwiler, B. H. & Charpak, S. (1998). Target cell specific modulation of transmitter release at terminals from a single axon. *Proceedings of the National Academy of Sciences of the USA* **96**, 12004–12009.

Schwartzkroin, P. A. & Prince, D. A. (1978). Cellular and field potential properties of epileptogenic hippocampal slices. *Brain Research* **147**, 117–130.

Shigemoto, R., Kinoshita, A., Wada, E., Nomura, S., Ohishi, H., Takada, M., Flor, P. J., Neki, A., Nakanishi, S. & Mizuno, N. (1997). Differential presynaptic localization of metabotropic receptor subtypes in the rat hippocampus. *Journal of Neuroscience* **17**, 7503–7522.

Spruston, N., Schiller, Y., Stuart, G. & Sakmann, B. (1995). Activity dependent action potential invasion and calcium influx into hippocampal CA1 dendrites. *Science* **268**, 297–300.

Stricker, C., Redman, S. & Daley, D. (1994). Statistical analysis of synaptic transmission: model discrimination and confidence limits. *Biophysical Journal* **67**, 532–547.

Welsh, J. P., Lang, E. J., Sugihara, I. & Llinas, R. (1995). Dynamic organisation of motor control within the olivo-cerebellar system. *Nature* **374**, 453–457.

Whittington, M. A., Traub, R. D. & Jefferys, J. G. R. (1995). Erosion of inhibition contributes to the progression of low magnesium bursts in rat hippocampal slices. *Journal of Physiology* **486**, 723–734.

Wilson, M. A. & MacNaughton, B. L. (1993). Dynamics of the hippocampal ensemble code for space. *Science* **261**, 1055–1058.

Acknowledgements

We gratefully acknowledge the assistance of Paula Parra in experiments to obtain the data for Fig. 2. We would like to thank P. Parra, N. Ankri, P. Faure, D. Fricker, G. Buzsáki, A. I. Gulyás and B. Barbour for helpful comments. This work was supported by INSERM and by grants from the HFSO and from the NIH (MH54671).

Corresponding author

R. Miles: Laboratoire de Neurobiologie Cellulaire, INSERM U261, Institut Pasteur, 25 rue de Dr Roux, 75724 Paris cedex 15, France.

Email: rmiles@pasteur.fr